Proceedings of the 11th Brazilian Congress of Thermal Sciences and Engineering – ENCIT 2006
Braz. Soc. of Mechanical Sciences and Engineering – ABCM, Curitiba, Brazil, Dec. 5-8, 2006

Paper CIT06-0703

Numerical Study of Turbulent Flow and Heat Transfer in a Rectangular Channel with Cubic-Shaped Pin-Fins

Paula M. B. Marinho
PEN/COPPE/UFRJ, Caixa Postal 68509, CEP 21941-972 - Ilha do Fundão, RJ
pmarinho@con.ufrj.br

Mariana R. do Carmo
PEN/COPPE/UFRJ, Caixa Postal 68509, CEP 21941-972 - Ilha do Fundão, RJ
marianarc@poli.ufrj.br

João F. Mitre
PEQ/COPPE/UFRJ, Caixa Postal 68502, CEP 21941-972 - Ilha do Fundão, RJ
mitre@peq.coppe.ufrj.br

Jian Su
PEN/COPPE/UFRJ, Caixa Postal 68509, CEP 21941-972 - Ilha do Fundão, RJ
sujian@con.ufrj.br

Paulo L. C. Lage
PEQ/COPPE/UFRJ, Caixa Postal 68502, CEP 21941-972 - Ilha do Fundão, RJ
paulo@peq.coppe.ufrj.br

Abstract. *Pin fins are widely used for convective heat transfer enhancement in compact heat exchangers, electronic circuits, gas turbine blades, etc. This paper reports a numerical study of the three-dimensional turbulent flow and heat transfer in a rectangular channel with cubic-shaped pin-fins mounted across the channel. Both inline and staggered arrangements of the pin-fins were investigated. The objective of this work was to develop and validate a numerical model of pin-finned channel flow that is able to reproduce available experimental data in the literature and thus can be used to evaluate other arrangements of the pin-finned channel. The numerical simulation was carried out by solving the Reynolds Averaged Navier-Stokes (RANS) equations with an advanced turbulent model, the Shear Stress Transport (SST) model, using a commercial CFD (Computational Fluid Dynamics) package ANSYS CFX 10.0. The numerical results of the stead-state heat transfer coefficient showed a good agreement with available experimental data.*

keywords: *CFD, turbulence models, pin-fin, heat exchanges, SST.*

1. Introduction

Pin fins heat exchangers are usually compounded by a large number of small pins with different geometries and arrangements to maximize the surface area for the heat transfer. Pin fin arrays are used to enhance convective heat transfer from an endwall in a variety of engineering applications. Early researches were motivated by the application of pin fins as heat transfer augmentation devices for cooling of gas turbine blades. Pin fin arrays are also used to increase heat transfer area in compact heat exchangers, in air-conditioning, in modern electronic devices, and more recently in solar absorbers. The pin fin heat transfer is highly sensitive to different geometries of the pins (cylindrical, cubic, diamond, etc) and to different arrangements (in-line, staggered, etc).

Forced convective heat transfer in pin finned channels have been a subject of extensive experimental studies. Armstrong and Winstanley, 1988 reviewed the heat transfer and flow friction data for staggered arrays of cylindrical pin fins in gas turbine cooling applications. Matsumoto *et al.*, 1998 analyzed experimentally the effect of pin-fin arrangements on endwall heat transfer. You and Chang, 1997 simulated numerically the heat transfer coefficient for a pin-fin channel flow. There are other studies done with cubic-shape pins. Chyu *et al.*, 1998 carried out an experiment of mass transfer to analyze the heat transfer by mass transfer analogy in a channel of cubic pin fins. Recently, Saha and Acharya, 2003 carried out a numerical study to analyze the unsteady three-dimensional turbulent and heat transfer in a parallel-plate channel heat exchanger with in-line arrays of periodically mounted rectangular pins at various Reynolds numbers and geometrical configurations.

Only one geometrically periodic domain is considered by imposing flow periodicity in order to save computational efforts. The unsteady Navier-Stokes equations are solved on a staggered grid by using a modified version of the MAC algorithm of Harlow and Welch, 1965. A minimum grid of $62 \times 62 \times 42$ and a maximum gird of $122 \times 122 \times 42$ were used. It was shown that the flow is three-dimensional for all configurations and unsteady in most of the cases above $Re = 180$. Mitre *et al.*, 2005 carried out numerical simulations of the turbulent heat transfer in a pin-finned channel with cylindrical geometry, using SST (Shear Stress Transport) turbulence model.

The purpose of this work is to analyze numerically the heat transfer and the fluid flow in a channel mounted with cubic-shaped pin fins. It has been found that a cubic element can produce greater heat transfer enhancement than a cylindrical pin (Chyu *et al.*, 1998). Following Mitre *et al.*, 2005, we simulated numerically the turbulent flow and heat transfer in the whole channel with 35 fins, without using periodic boundary conditions. A channel with inline and staggered arrangement was simulated. The SST (Shear Stress Transport) turbulence model is used for the Reynolds stress closure (Menter, 1993, Menter, 1994, Menter *et al.*, 2003). Our objective is to reproduce numerically the experimentally obtained the heat transfers coefficients available in the literature.

2. Experimental Validation

The validation of the numerical simulations was based on the experimental work of Chyu *et al.*, 1998, which studied the heat transfer in arrays with cubic and diamond pin-fins in inline and staggered arrangements. Chyu *et al.*, 1998 used the mass transfer analogy for the the heat transfer measurement and analyzed the behavior of a fluid in a channel compounded by a large number of small cubic pins. The cubes had 12.5 mm of edge (D) and $S = X = 2.5D$. They were disposed of two forms: in a align array were seven rows of five elements and in a staggered were seven rows of four or five elements. The channel had a rectangular cross section of 159 mm width and 12.5 mm height (equal to D). It had a hydraulic diameter (D_h) was 23.5 mm. The initial portion of the channel serves as the hydrodynamic development section and delivers the flow to the test section. The geometrical configuration of the pin-finned channel is shown in Fig.(1).

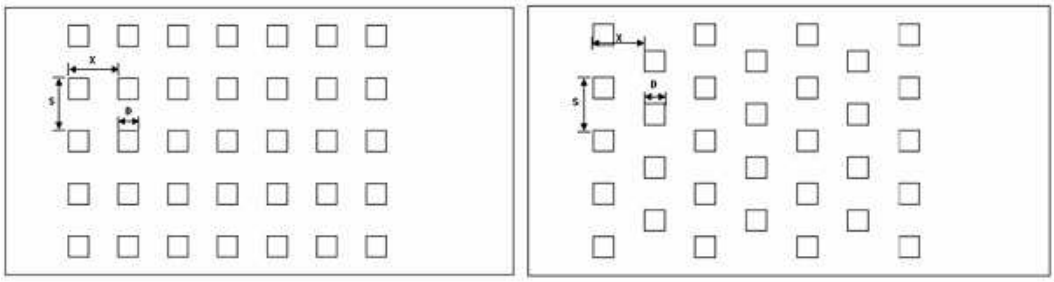

Figure 1: Cut view of pin-fin channel: inline channel and staggered channel

It was developed an experiment of mass transfer and study heat transfer by analogy. In this experiment, aluminum fins were covered with naphthalene. This was achieved by dipping the cube into molten naphthalene. A nearly 0.5 mm thick layer formed on the cube surface. Then, all the fins are separately weighed with 0.01 mg of accuracy in a 166 g range. The cubes were mounted on the wall, according to the geometry. Then, dry air was blown inside the finned channel for 30 minutes. The temperature was determined, during the experience, by the average of the readings of four thermocouple sensors embedded in the inner surface of the two finned walls of the channel. The results were rejected if, at least, two of the four sensors had registered a temperature difference of more than 0.2 C. After the test, all the fins were unmounted and weighed again. The lost weight was the amount of naphthalene sublimed during the test run. The average naphthalene mass sublimed was approximately 30 mg.

With the total mass of naphthalene before and after the experiment, it is possible to calculate the mass transfer coefficient. So, it is also possible to calculate the heat transfer coefficient by analogy. In the test the temperature was constant, therefore, fluid properties remain constant too.

It was assumed, in this simulation, that the fluid was air with temperature of 25 ^{o}C e pressure of 1 atm with Prandtl number equal to 0.7.

3. Mathematical Modeling

For the mathematical model, we considered three dimensional, transient, turbulent flow of a Newtonian fluid with constant thermophysical properties. The continuity equation is:

$$\nabla \bullet \mathbf{U} = 0 \tag{1}$$

where ρ is the specific mass, $\mathbf{U}$ is the velocity vector and t is the time. The Reynolds averaged Navier-Stokes (RANS) equations are given by:

$$\frac{\partial \rho \mathbf{U}}{\partial t} + \nabla \bullet (\rho \mathbf{U} \otimes \mathbf{U}) - \nabla \bullet (\mu_{eff} \nabla \mathbf{U}) = \nabla p' + \nabla \bullet (\mu_{eff} \nabla \mathbf{U})^T + \mathbf{B} \tag{2}$$

where $\mathbf{B}$ is the body force vector, that is null in this study, μ_{eff} is the effective viscosity and p' is turbulent modified pressure.

The turbulent modified pressure is defined by:

$$p' = p + \frac{2}{3}\rho k \tag{3}$$

where p is pressure, k is the turbulence kinetic energy.

The effective viscosity is given by:

$$\mu_{eff} = \mu + \mu_t \tag{4}$$

where μ_t is the turbulent eddy viscosity and μ is the molecular viscosity of the fluid.

The Reynolds averaged energy equation, considering an incompressible fluid with constant specific heat, is defined by:

$$\rho c_p \frac{\partial T}{\partial t} + \rho c_p \nabla \bullet \mathbf{U} T = \nabla \bullet \left(\left(\lambda + \frac{c_p \mu_t}{\mathbf{Pr}_t} \right) \nabla T \right) + \mathbf{S}_E \tag{5}$$

where c_p is the specific heat, T is the temperature, λ is the thermal conductivity, $\mathbf{Pr}_t$ is the turbulent Prandtl number, assumed to be 0.9, and $\mathbf{S}_E$ is the thermal source term, which is null, in this study.

In this work, we employed the SST turbulence model - *Shear Stress Transport* (Menter, 1993, Menter, 1994, Menter *et al.*, 2003) which is indicated for calculation of skin friction and heat flow at solid surface. This model uses the $k-\omega$ near the wall and uses the $k-\epsilon$ far from the wall, where each one gives the better results.

The transformed equations for the $k-\epsilon$ and the $k-\omega$ for SST turbulence model are:

$$\frac{\partial (\rho k)}{\partial t} + \nabla \bullet (\rho \mathbf{U} k) = \nabla \bullet \mu + \mu_t \sigma_k \nabla k + \widetilde{P}_k - \beta^* \rho \omega k \tag{6}$$

$$\frac{\partial \rho \omega}{\partial t} + \nabla \bullet \rho \mathbf{U} \omega = \nabla \bullet \mu + \mu_t \sigma_\omega \nabla \omega + 2(1 - F_1) \rho \sigma_{\omega 2} \frac{1}{\omega} \nabla k \bullet \nabla \omega + \frac{\alpha}{\nu_t} P_k - \beta \rho \omega^2 \tag{7}$$

where ω is the turbulence frequency and $\nu_t = \mu_t / \rho . P_k$ is the shear production of turbulence and its limits are defined by:

$$P_k = \tau : \nabla \mathbf{U} \quad \rightarrow \quad \widetilde{P}_k = \min(P_k, 10 \beta^* \rho k \omega) \tag{8}$$

where the Reynolds stress tensor is given by $\tau = 2\mu_t \mathbf{D} - \frac{2}{3}\rho k \delta$, where $\mathbf{D} = \frac{1}{2}\nabla \mathbf{U} + \nabla \mathbf{U}^T$.

All the model constants are obtained by combination the corresponding constants of the $k-\epsilon$ and $k-\omega$ model using a blending function F_1 by $\alpha = \alpha_1 F_1 + \alpha_2 (1 - F_1)$, where α_1 e α_2 are the constants of the models $k-\omega$ and $k-\epsilon$ respectively.

The constants for this model are: $\beta^* = 0,09$, $\alpha_1 = 5/9$, $\beta_1 = 3/40$, $\sigma_{kl} = 0,85$, $\sigma_{\omega l} = 0,5$, $\alpha_2 = 0,44$, $\beta_2 = 0,0828$, $\sigma_{k2} = 1$ e $\sigma_{\omega 2} = 0,856$.

The first blending function F_1 is defined by:

$$F_1 = \tanh\left\{ \left\{ \min\left[\max\left(\frac{\sqrt{k}}{\beta^* \omega y}, \frac{500\nu}{y^2 \omega} \right), \frac{4\rho\sigma_{\omega 2} k}{CD_{k\omega} y^2} \right] \right\}^4 \right\} \tag{9}$$

where $CD_{k\omega}$ is

$$CD_{k\omega} = \max\left(2\rho\sigma_{\omega 2} \frac{1}{\omega} \nabla k \bullet \nabla \omega, 10^{-10} \right) \tag{10}$$

which y is the distance to the nearest wall.

F_1 is equal to zero away from the surface ($k-\epsilon$ model), and switches to one inside the boundary layer ($k-\omega$ model). The turbulent eddy viscosity is defined as:

$$\nu_t = \frac{a_1 k}{\max(\quad a_1 \omega, SF_2)} \tag{11}$$

where $a_1 = 0,31$, S is the invariant measure of strain rate given by $\sqrt{2\mathbf{D}:\mathbf{D}}$ and F_2 is a second blending function defined by:

$$F_2 = \tanh\left[\left[\max\left(\frac{2\sqrt{k}}{\beta^*\omega y}, \frac{500\nu}{y^2\omega}\right)\right]^2\right] \tag{12}$$

This model requires the knowledge of the distance between the nodes and the nearest wall. So, it is obtained a better interaction between the $k-\omega$ and $k-\epsilon$. The wall scale equation is solved to get these wall distances:

$$\nabla^2\phi = -1 \tag{13}$$

where ϕ is the value of the wall scale. The wall distance can be calculated from the wall through:

$$WD = \sqrt{|\nabla\phi|^2 + 2\phi - |\nabla\phi|} \tag{14}$$

The mathematical model is solved numerically by using the commercial CFD package *ANSYS CFX-10.0*. This program uses numerical method of finite volume as solution (Element Based Finite Volume Method - EBFVM), which allows the solution of problems by blending of unstructured grids. Then, it is possible to obtain a numerical solution of discretized momentum and mass balance equations.

4. Computational Domain, Grid and Bondary Conditions

The computational domain consists of a channel with 40 mm long section before the first line of pins and 80 mm section after the last line of pins, resulting in a channel length of 320 mm. The cross section of the channel has a width of 159.0 mm and a height of 12.5mm. The channel has a hydraulic diameter (D_h) of 23.5 mm.

The hydraulic diameter (D_h) is a parameter of Reynolds number:

$$Re_D = \frac{\rho U_\infty D_h}{\mu} \tag{15}$$

where U_∞ is an average velocity of gas on inlet.

Two meshes were used, one for the inline configuration and other for the staggered configuration. Hybrid meshes were used in the two geometries . The meshes were compounded by wedges and hexahedral elements. They were extruded with 20 elements in the channel height direction, from the extremities to the center. In the two extrusions had a symmetric refinement near the upper and lower channel walls with a grown rate of 1.2. The global size of the meshes was 1 mm. It is possible to observe in Fig.(2), that shown the mesh of the staggered geometry.

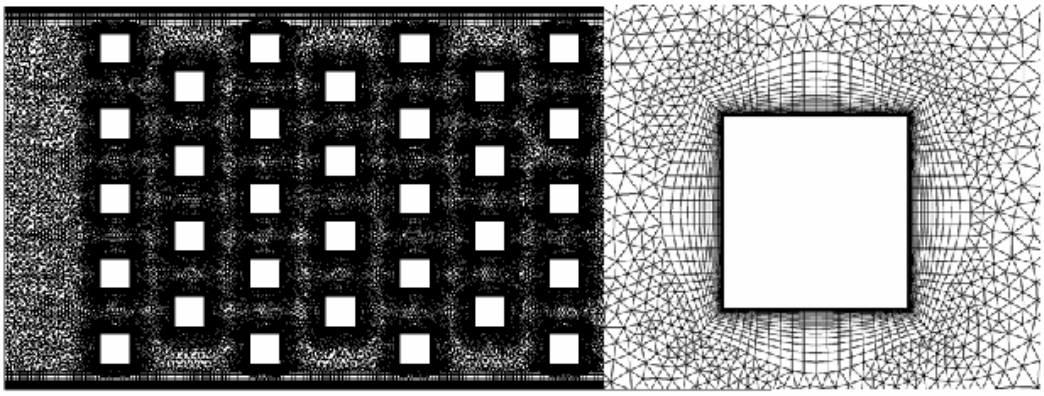

Figure 2: Mesh cut view and near fin mesh refinement

The refinement on the fins surfaces was in the normal direction of each surface. It consisted of 20 layers whose thickness grew at a factor of 1.2 away from the surface. In general, the meshes had about 2500000 nodes.

In the channel inlet, it was assumed a flow with constant velocity, as a function of the Re_D according to experimental data, and the temperature of 25 C. The channel walls were considered adiabatic and fins walls had a constant temperature of 30 C and non-slip conditions for the velocity.

At the channel outlet, the boundary condition called *Opening* by the CFX code was used. This condition consists in the prescription of a mean average relative static pressure (null, in this case) with the possibility of reflux. So it is possible to define a short downstream domain, which reduces the mesh size. In case of reflux, the inflow fluid temperature was set to be the mean outlet temperature.

5. Results

The simulations were carried out in parallel (using the MPICH parallelization library) with 4 Pentium 4 processors at 3 GHz and 2,3 Gb of RAM memory. The steady state convergence was reached in approximately 150 iterations, with the residual criteria (RMS value of the normalized residuum of each mesh node) of $10^{-}3$. The simulation took about 24 hours on this cluster to approximately 700 iterations, in order to better observations about of simulation.

All results for the Nusselt number were in good agreement with the experimental data, as can be seen in Fig.(3). The largest relative deviation in Nusselt number was approximately 10%, which occurred for the highest Reynolds number simulation with the staggered arrangement.

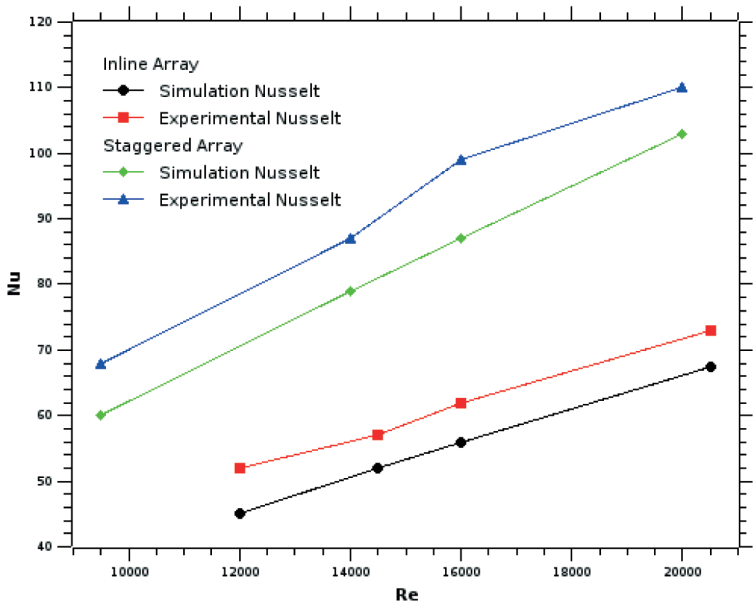

Figure 3: Comparison between the experimental and simulated Nusselt number data

Some difficulties were encountered in carrying out these simulations. The principal difficulty is the unstable character of the flow around the pins. The observed flow pattern clearly characterizes transient flow. Since the magnitude of these flow instabilities were sufficiently small, steady state solutions could be obtained for the not too strict convergence criterion used. Although a transient solution would be a better representation of the flow in these pin-fin channels, the steady state solution sufficed for Nusselt number evaluation and it saved a lot of computational time.

Figures(4) to (9), shown below, were computed for Reynolds number values of 16,000 for the in-line array and the staggered array, in order to minimize the effect off velocity in comparative analysis between configurations

It can be observed in Fig. (4) that no symmetry in velocity contours is encountered. A perfect steady state solution would not have this non-symmetrical appearance. This behavior is also shown in the Fig. (5), which present the heat rates along the solver iterations for each fin. For a perfect steady state solution, all the heat rate values should be constant. Figure (6) show the total heat transfer rates (in all fins). It is clear that their convergence is better.

It can be also observed in Fig. (7) a non simmetric contour for the temperature profile.

Figure(8) shows the streamlines near to the pins colored according to the velocity value. An unstable vortex can be clearly observed in this figure. Figure(9) shows the values of dimensionless normal distance of the nearest grid point to the fin wall, $y_1^+ (= u_\tau \Delta y_1/\nu)$, with a maximum observed value of 3.9.

6. Conclusions

CFX steady-state simulations using SST turbulence model were employed to evaluate the heat transfer in pin-finned channel inline and staggered configurations. It can be concluded from the numerical simulations the the turbulent flow in a pin-finned channel is an unstable phenomenon and there is not a steady-state solution. However, the amplitude of the oscillations is less than the coefficient lagging, therefore, the steady-state simulations on CFX converge to a quasi-steady regime. For the conditions analyzed in the work, the flows through the pin-finned channels reached quasi-periodic regimes. The total heat transfer rates were evaluated, whose values

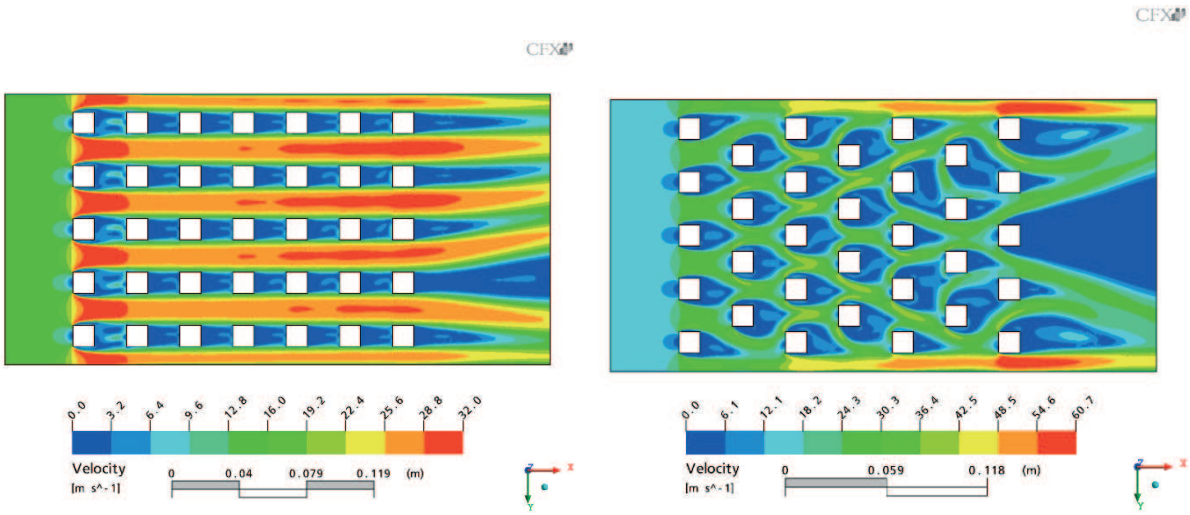

Figure 4: Velocity contours at mid-height: inline and staggered arrays

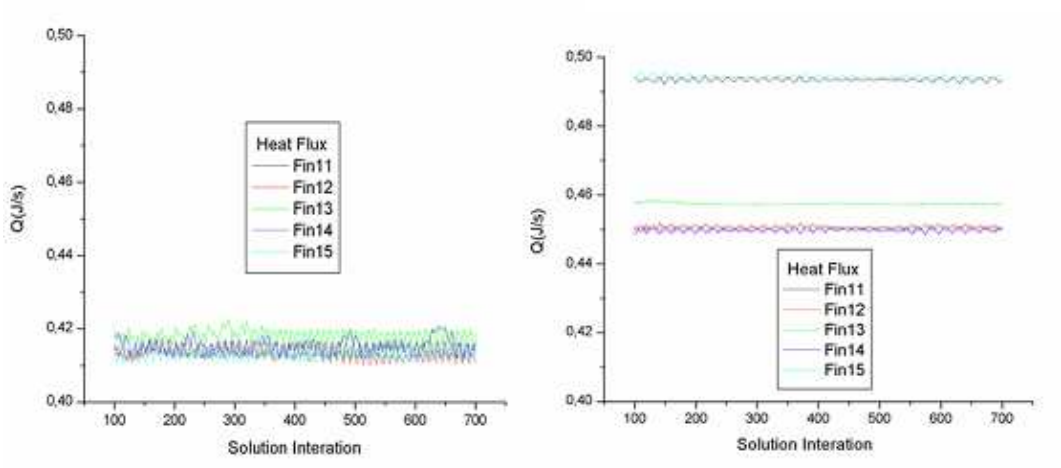

Figure 5: Heat flux in the fins: inline and staggered arrays. The matrix index Fin_ij represents the fin at line i and column j.

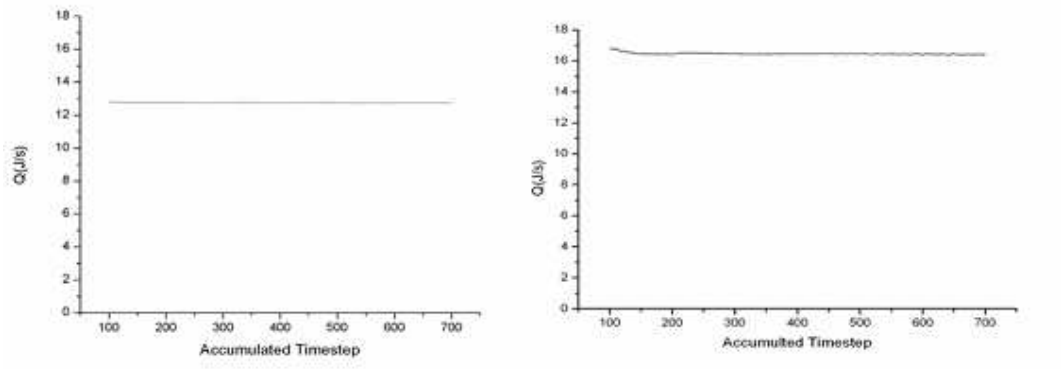

Figure 6: Total heat flux in all fins: inline and staggered arrays.

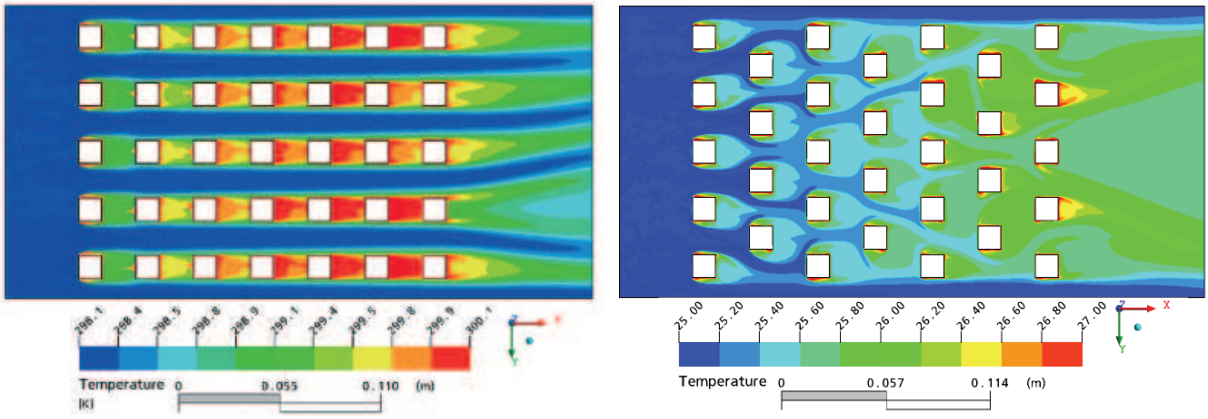

Figure 7: Temperature contours at mid-height: inline and staggered arrays.

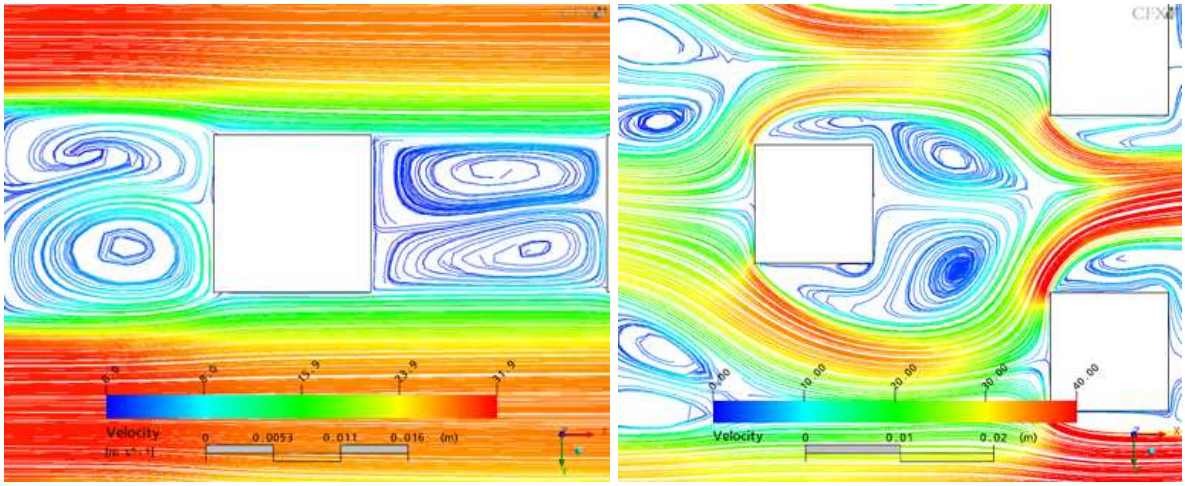

Figure 8: Velocity streamlines at mid-height: inline and staggered arrays.

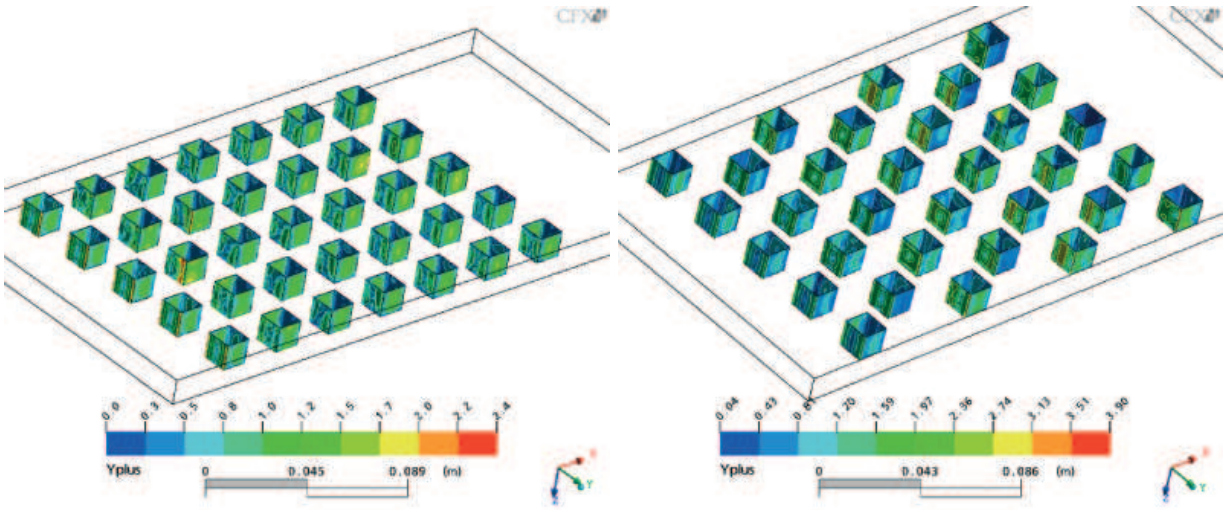

Figure 9: Contours of y_1^+ values: inline and staggered arrays.

oscillated much lesser than the fin heat transfer rates due to out of phase behavior of the latter. Therefore, the global Nusselt numbers could be evaluated with good accuracy from the CFX steady-state simulations and their values compared favorably to the available experimental data. Although transiente simulations should be used to investigate deeper the velocity and temperature fields, the performace of the SST turbulence model in prediction the global heat transfer rate can be regarded as very good.

7. Acknowledgements

The authors would like to acknowledge the support of CNPq, CAPES and FAPERJ for the realization of the work.

8. References

Armstrong, J. and Winstanley, D., 1988, A Review of Staggered Array Pin Fin Heat Transfer for Turbine Cooling Applications, "Transations of the ASME Journal of Turbomachinery", Vol. 110, pp. 94–103.

Chyu, M. K., Hsing, Y. C., and Natarajan, V., 1998, Convective Heat Transfer of Cubic Fin Arrays in a Narrow Channel, "Transations of the ASME Journal of Turbomachinery", Vol. 120, pp. 362–367.

Harlow, F. H. and Welch, J. E., 1965, Numerical calculation of time-dependent viscous incompressible flow of fluid with free surfaces, "Phys. Fluids", Vol. 8, pp. 2182–2188.

Matsumoto, R., Kikkawa, S., and Senda, M., 1998, Effect of Pin Fin Arrangement on Endwall Heat Transfer, "JSME International Journal", Vol. 40, pp. 142–151.

Menter, F. R., 1993, Zonal two-equation $k-\omega$ turbulence model for aerodynamic flows, AIAA Paper 1993-2906.

Menter, F. R., 1994, Two-equation eddy-viscosity turbulence models for engineering applications, "AIAA Journal", Vol. 32, pp. 269–289.

Menter, F. R., Kunz, M., and Langtry, R., 2003, Ten years of industrial experience with the SST turbulence model, "Turbulence, Heat and Mass Transfer 4, K. Hanjalic, Y. Nagano and M. Tummers (eds.)", Begell House.

Mitre, J. F., Damian, R. B., Lage, P. L. C., and Su, J., 2005, Numerical Simulation of the Turbulent Heat Transfer in a Pin-Finned Channel, "Proceedings of 18th Int. Congress Mech. Eng. (COBEM2005)", Ouro Preto, MG, Brazil.

Saha, A. K. and Acharya, S., 2003, Parametric study of unsteady flow and heat transfer in a pin-fin heat exchanger, "International Journal of Heat and Mass Transfer", Vol. 46, pp. 3815–3830.

You, H. I. and Chang, C. H., 1997, Numerical Prediction of Heat Transfer Coefficient for a Pin-Fin Channel Flow, "Transactions of the ASME Journal of Heat Transfer", Vol. 119, pp. 840–848.